

Critical conductance of a one-dimensional doped Mott insulator

M. Garst,¹ D. S. Novikov,² Ady Stern,³ and L. I. Glazman²

¹*Institut für Theoretische Physik, Universität zu Köln, 50938 Köln, Germany*

²*W. I. Fine Theoretical Physics Institute, University of Minnesota, Minneapolis, MN 55455, USA*

³*Department of Condensed Matter Physics, Weizmann Institute of Science, Rehovot 76100, Israel*

(Dated: January 22, 2008)

We consider the two-terminal conductance of a one-dimensional Mott insulator undergoing the commensurate-incommensurate quantum phase transition to a conducting state. We treat the leads as Luttinger liquids. At a specific value of compressibility of the leads, corresponding to the Luther-Emery point, the conductance can be described in terms of the free propagation of non-interacting fermions with charge $e/\sqrt{2}$. At that point, the temperature dependence of the conductance across the quantum phase transition is described by a Fermi function. The deviation from the Luther-Emery point in the leads changes the temperature dependence qualitatively. In the metallic state, the low-temperature conductance is determined by the properties of the leads, and is described by the conventional Luttinger-liquid theory. In the insulating state, conductance occurs via activation of $e/\sqrt{2}$ charges, and is independent of the Luttinger-liquid compressibility.

PACS numbers: 71.27.+a 71.10.-w 73.43.Nq 73.21.Hb

I. INTRODUCTION AND OUTLINE

The dc conductance of a one-dimensional (1D) system crucially depends on the properties of the leads attached to it. Unlike in higher dimensions, this dependence is not merely a technological, but rather a generic physics problem.

In the case of the conventional Luttinger-liquid model for a quantum wire,¹ the role of the leads in the zero-temperature ($T = 0$) conductance is well studied.^{1,2,3,4,5} As long as the electrons do not backscatter off inhomogeneities, the conductance is not sensitive to the nature of carriers in the wire, and is determined solely by the leads. In the simplest case of the noninteracting leads, the conductance is quantized in units of $e^2/2\pi\hbar$ per channel (each of the two spin polarizations counts for a separate channel). This conclusion also remains true for the incommensurate phase of a so-called Mott wire (doped 1D Mott insulator).^{6,7} Thus the charge fractionalization characteristic of these systems^{1,8} is not observable in the zero-temperature ballistic conductance; if the leads are Fermi liquids, then the ballistic conductance of the wire appears to coincide with that of the free electrons.⁹

The Tomonaga-Luttinger model is applicable to a relatively dense system of particles forming a compressible liquid. The “distance” from the incompressible state may be characterized by a parameter $-r$, having the meaning of chemical potential measured from the point where the system becomes incompressible. For example, for free fermions filling up a conduction band

$$-r \equiv \mu - \Delta \quad (1.1)$$

with μ and Δ being the Fermi energy and band edge, respectively. At $T = 0$ and $\mu < \Delta$ the system is incompressible.

The conventional Luttinger liquid model requires relatively high carrier density, $-r/T \gg 1$. How robust is the

apparent free-electron picture of transport if the condition $-r/T \gg 1$ is violated? One may expect deviations from the apparent free-fermion form of the two-terminal conductance in some intermediate region of parameters¹⁰ in a conventional quantum wire. However, for fully spin-polarized electrons (equivalent to spinless fermions) at the point $r = 0$ of the quantum phase transition the interaction becomes irrelevant. The corresponding conductance equals $\frac{1}{2} \times e^2/h$, i.e. a half of the unit conductance quantum e^2/h for spinless fermions, which is again indistinguishable from a free-fermion result.¹¹

Charge carriers at the commensurate-incommensurate quantum phase transition in a Mott wire can also be mapped onto free spinless fermions.⁷ The distance to the phase transition is characterized by a chemical potential $-r$, see Eq. (1.1), here measured with respect to the Mott gap, Δ . However, these effective fermions have fractional charge, and are related to the original electrons in a complicated way. It is therefore an important unresolved question as to what the two-terminal critical conductance of a Mott wire is.

The aim of this work is to investigate the finite-temperature conductance around the quantum phase transition point in a Mott wire. Our main finding is that such a setup may provide the way to experimentally access the elusive character of the fractional quasiparticle charge in an interacting 1D system.

To be specific, we consider the two-terminal conductance of a one-dimensional electron system close to the Mott transition. The details of how the underlying commensuration is realized in practice, e.g. by a periodic potential, will not be important; the only parameter from the Mott wire we will need in the end is the effective value Δ of the charge gap. Next, we assume that this wire is smoothly attached to uniform identical Luttinger liquid leads characterized by the Luttinger parameter K_L . We evaluate the finite-temperature conductance close to the Mott transition perturbatively in $K_L - \frac{1}{2}$. The value of

$K_L = \frac{1}{2}$ is special (Luther-Emery point¹²), as it allows a mapping of the entire system onto a free-fermion one. In lowest order in $K_L - \frac{1}{2}$, we find

$$\frac{G}{G_0} = \frac{1}{2}f(r/T) + \left(K_L - \frac{1}{2}\right)f^2(r/T), \quad G_0 = \frac{2e^2}{h}, \quad (1.2)$$

where r is the tuning parameter (1.1) of the Mott transition, G_0 is the conductance quantum, and

$$f(x) = \frac{1}{1 + e^x} \quad (1.3)$$

is the Fermi function. On the metallic side, $r < 0$, the conductance approaches the value $K_L G_0$ in the limit of zero temperature, i.e., it is determined by the Luttinger liquid parameter of the leads in agreement with Ref. 6. On the other hand, on the insulating side of the transition, $r > 0$, transport at low T is thermally activated as the Fermi function reduces to a Boltzmann factor, $f(r/T) \approx e^{-r/T}$. In lowest order in the fugacity $e^{-r/T}$, we find that the conductance $G = \frac{1}{2}G_0 e^{-r/T}$ is not affected by the leads, i.e., is independent of K_L . In particular, the prefactor of the exponential is determined by the effective conductance quantum $\frac{1}{2}G_0$ attributed to the degrees of freedom of the critical Mott wire. As we will explain in detail below, the critical degrees of freedom are the fermions that carry fractional charge

$$e_{\text{CI}} = e/\sqrt{2}. \quad (1.4)$$

At low temperatures transport in the Mott insulator occurs via activation of the fractional charges (1.4), resulting in the announced prefactor $\frac{1}{2}G_0 \equiv 2e_{\text{CI}}^2/h$. Finally, in the extended quantum critical regime, $|r| \ll T$, the conductance is dominated by its critical value,

$$G_{\text{cr}} \equiv G|_{r=0} = \frac{2K_L + 1}{8}G_0 + \mathcal{O}(K_L - \frac{1}{2})^2. \quad (1.5)$$

Note that the specific fraction of the conductance quantum here depends both on the fractional charge of the carriers and on the properties of the leads. These results differ from the considerations of Mori *et al.*⁷

Our study of the two-terminal conductance of the critical Mott insulator complements the theoretical investigation of ballistic transport in massive theories in general, for a recent review see Ref. 13. The thermally activated quasiparticles above a gapped ground state in a homogeneous system (no leads) may travel ballistically thus giving rise to a singular contribution to the optical conductivity, $\sigma_{\text{sing.}}(\omega) = 2\pi D\delta(\omega)$, with a characteristic Drude weight $D = D(T)$. The low-temperature Drude weight of the Mott insulator is believed to remain finite even away from criticality.¹⁴ (In the exact commensurate case of an undoped Mott insulator the fate of the Drude weight is less clear and remains a subject of ongoing research.^{15,16}) Remarkably, the knowledge of the Drude weight in the conductivity of a uniform 1D system is insufficient for

finding its two-terminal dc conductance. The latter is affected by the different nature of the charge carriers in the leads and in the wire.

The paper is organized as follows. In Section II we consider the properties of the uniform Mott wire. In Section III we consider the Mott wire with the leads, and evaluate the modification of the critical conductance induced by the presence of the leads. Section IV is devoted to the discussion of our results.

II. UNIFORM MOTT WIRE

In this Section we consider the model of the uniform 1D Mott wire. In Sec. II A we introduce the Hamiltonian of our system, and in Sec. II B we sketch the critical theory describing the Mott transition. In Sec. II C we outline the application of the Kubo formula for the calculation of conductance, and derive the critical conductance for the Mott wire without leads in Sec. II D.

A. Model of the one-dimensional Mott insulator

Consider an interacting one-dimensional electron system in the vicinity of the Mott transition. The latter can be realized, e.g., in a Hubbard model close to half-filling. The effective Hamiltonian is conventionally represented in terms of the bosonic charge and spin excitations that decouple at sufficiently low energies.⁸ In this work we only focus on the charge sector which, near the transition, is described by the sine-Gordon model⁸

$$\mathcal{H}[\phi_c, \theta_c] = \int \frac{dx}{2\pi} \left[Ku(\partial_x \theta_c)^2 + \frac{u}{K}(\partial_x \phi_c)^2 \right] + \int dx \frac{2V_{\text{Uml}}}{(2\pi a)^2} \cos(\sqrt{8}\phi_c - q_0 x). \quad (2.1)$$

Here K is the Luttinger parameter, u is the plasmon velocity, V_{Uml} is the Umklapp scattering amplitude (given by the Fourier component of the lattice potential at the reciprocal lattice vector) that corresponds to g_3 in the standard g -ology classification,⁸ and a is a short distance cutoff. The conjugate fields ϕ_c and θ_c , with $[\frac{1}{\pi}\partial_x \phi_c(x), \theta_c(x')] = -i\delta(x - x')$, describe the smooth components of the density and current fluctuations within the system,

$$\delta n = -\sqrt{2} \frac{\partial_x \phi_c}{\pi}, \quad \text{and} \quad j = \sqrt{2} K u \frac{\partial_x \theta_c}{\pi}, \quad (2.2)$$

respectively. The prefactor $\sqrt{2}$ in these expressions is attributed to the two spin polarizations of the electrons. The parameter q_0 measures the distance to half-filling. In the presence of repulsive interaction between the electrons, $K < 1$, the umklapp scattering process, V_{Uml} , becomes relevant and opens up a gap in the spectrum at half filling $q_0 = 0$, rendering the system into the Mott insulating phase.

The elementary excitations of the Mott insulator are massive quantum solitons (kinks) of the model (2.1). Classically, the kink must connect two discrete values of $\phi_c(x \rightarrow \pm\infty)$, which realize the minimum of the cosine term. This dictates the *fractional* value of the topological charge

$$Q = \frac{1}{\pi} \int_{-\infty}^{\infty} dx \partial_x \phi_c^{\text{soliton}}(x) = \frac{1}{\sqrt{2}}. \quad (2.3)$$

Below we will absorb the topological charge (2.3) carried by the solitons into the fractional electric charge quantum, $e_{\text{CI}} = Qe$, cf. Eq. (1.4).

Upon detuning the system from half-filling by increasing q_0 across a critical value the system becomes conducting via the commensurate-incommensurate (CI) transition.^{8,17} The ground state of this conducting phase is characterized by a finite topological charge density. Consequently, this transition is described^{18,19} by exploiting the duality^{20,21} between the sine-Gordon model (2.1) and the massive Thirring model. To establish this duality, we make a canonical transformation to the rescaled fields

$$\phi = \sqrt{2}\phi_c, \quad \text{and} \quad \theta = \theta_c/\sqrt{2}. \quad (2.4)$$

In these variables the model (2.1) becomes

$$\begin{aligned} \mathcal{H}[\phi, \theta] = & \int \frac{dx}{2\pi} \left[2Ku(\partial_x \theta)^2 + \frac{u}{2K}(\partial_x \phi)^2 \right] \\ & + \int dx \frac{2V_{\text{UmkI}}}{(2\pi a)^2} \cos(2\phi - q_0 x). \end{aligned} \quad (2.5)$$

The above Hamiltonian for the charge sector can now be refermionized with the help of the standard bosonization formula,

$$\psi_\kappa = \frac{1}{\sqrt{2\pi a}} e^{-i\kappa\phi + i\theta}, \quad (2.6)$$

with $\kappa = +1$ and -1 for right (R) and left (L) movers, respectively. The fermionic particles associated with the operator ψ_κ are identified with the solitonic excitations of the sine-Gordon theory; the fermionic density thereby coincides with their topological charge density. The resulting fermionic theory is the massive Thirring model,

$$\begin{aligned} \mathcal{H}[\Psi] = & \int dx \left\{ \Psi^\dagger [-iv\sigma^3 \partial_x - \mu + \sigma^1 \Delta] \Psi \right. \\ & \left. + \frac{1}{4}(g_4 + g_2)(\Psi^\dagger \Psi)^2 + \frac{1}{4}(g_4 - g_2)(\Psi^\dagger \sigma^3 \Psi)^2 \right\} \end{aligned} \quad (2.7)$$

where σ^i are the Pauli matrices, and we used the spinor notation $\Psi^\dagger = (\psi_R^\dagger, \psi_L^\dagger)$ for the new *spinless* fermions. As the Fermi momentum for the fictitious Dirac fermions Ψ is set to zero (at the Dirac point), there are no spatially oscillating factors in Eq. (2.6). These fermions (or the solitonic excitations of the sine-Gordon theory) describe the density excitations smooth on the scale of the original lattice responsible for the Mott phase. The parameters

of the model (2.7) are the chemical potential $\mu = -vq_0/2$ and the gap $\Delta = V_{\text{UmkI}}/(2\pi a)$,²² the velocity v and the interaction constants g_4 and g_2 are implicitly given by

$$u = v \sqrt{(1 + \nu g_4)^2 - (\nu g_2)^2}, \quad (2.8)$$

$$2K = \sqrt{\frac{1 + \nu g_4 - \nu g_2}{1 + \nu g_4 + \nu g_2}}, \quad (2.9)$$

where the density of states for the Ψ -fermions

$$\nu = \frac{1}{2\pi v}. \quad (2.10)$$

Note the redundancy of the g_4 interaction as it enters the mapping only in combination with the velocity, $2\pi v + g_4$. We deliberately choose to keep both the g_2 and g_4 interaction constants, as it will help us later to classify different perturbative contributions to the conductivity. The Luttinger interaction parameter for the new fermions (2.7) is $2K$. As a result, the interaction among them vanishes at the Luther-Emery point,¹² $K = \frac{1}{2}$. Later, in Section III we will apply the above formalism to the wire with the leads, and develop a perturbative expansion around this special value for the Luttinger parameter within the leads, K_L .

In terms of the spinless fermionic degrees of freedom the charge current density, $J = ej$, is given by

$$J = \sqrt{2}eKu \frac{\partial_x \theta_c}{\pi} = \sqrt{2}e_{\text{CI}} \Psi^\dagger v_J \sigma^3 \Psi. \quad (2.11)$$

Again, the overall multiplicative factor $\sqrt{2}$ can be traced back to the spin degree of freedom of the original electrons. As announced, we absorbed the topological charge associated with the fermions, $Q = 1/\sqrt{2}$, into the fractional electric charge quantum, $e_{\text{CI}} = Qe$, of Eq. (1.4). Moreover, the charge velocity of the new fermions reads

$$v_J = v(1 + \nu g_4 - \nu g_2). \quad (2.12)$$

For the general case $g_2 \neq g_4$, the velocity v_J depends on the interactions (cf. Ref. 8, Sec. 7.2).

The quadratic part of the refermionized theory (2.7) can be diagonalized by a Bogoliubov transformation resulting in the two bands with the spectrum $\pm\epsilon_k$, where $\epsilon_k = \sqrt{\Delta^2 + (vk)^2}$. When the chemical potential lies within the gap, $|\mu| < \Delta$, the ground state is a Mott insulator. When the chemical potential is tuned into one of the two bands the ground state becomes a conductor via the CI transition.

B. Critical theory of the commensurate-incommensurate Mott transition

From now on in this work we will focus on the properties of the system close to the Mott transition and assume in the following that the chemical potential of the Ψ fermions is near the upper band edge, $\mu \approx \Delta$, i.e.,

$r \approx 0$, where r is the tuning parameter for the quantum phase transition, cf. Eq. (1.1). The generalization to the situation when $\mu \approx -\Delta$ is straightforward and will not be further discussed.

The effective Hamiltonian governing the transition is given by nonrelativistic free spinless fermions,^{18,19}

$$\mathcal{H}_{\text{CI}} = \int dx c^\dagger(x) \left[r - \frac{\partial_x^2}{2m} \right] c(x), \quad (2.13)$$

where the operator c^\dagger creates a fermionic excitation in the upper band, the mass is $m = \Delta/v^2$, and r is defined in Eq. (1.1). The scaling dimension of the tuning parameter and the critical dynamical exponent are $\dim[r] = 1/\nu_r = 2$ and $z = 2$, respectively.

As the gas of fermions is very dilute at the transition, their interaction is weak. As the CI transition is approached, $r \rightarrow 0$, the interaction among the fermions decreases faster than their density, rendering the c fermions free at the transition. Speaking crudely, the fermions are free not because they do not interact *per se* but because there are too few particles to interact with. Formally, this can be seen from considering the residual interaction

$$\mathcal{H}_{\text{int}}^{\text{CI}} = \frac{1}{4} \sum_{kk'pp'} \delta_{k+k', p+p'} \Gamma_{kk'; pp'} c_k^\dagger c_{k'}^\dagger c_p c_{p'}. \quad (2.14)$$

The interaction amplitude $\Gamma_{kk'; pp'}$ is strongly constrained as the Pauli principle requires the effective amplitude to be antisymmetric upon exchange of momenta $p \leftrightarrow p'$ and $k \leftrightarrow k'$. Near the CI transition we can expand the amplitude, and the lowest order contribution is suppressed by two powers of momenta,

$$\Gamma_{kk'; pp'} = \gamma(k - k')(p - p'), \quad (2.15)$$

with the coefficient $\gamma = -g_2 v^2 / (4\Delta^2)$. As a consequence, at the quantum critical point the residual interaction, γ , is irrelevant in the renormalization group sense.

The phase diagram of the CI Mott transition is shown in Fig. 1. The tuning parameter r controls the distance to the quantum critical point; for $r > 0$ the system is in the commensurate phase with an insulating ground state. In the metallic phase, $r < 0$, at lowest temperatures $T < T_{\text{LL}}$, with $\log(|r|/T_{\text{LL}}) \propto 1/|r|$, a crossover between the critical behavior and the Luttinger liquid takes place; the residual interaction γ at finite density induces Luttinger liquid correlations in the spectral function of the c fermions with the Luttinger parameter $K_c - 1 \propto \sqrt{|r|}$.

C. Transport

We will consider electric transport through the critical Mott wire. Like the thermodynamic properties, the transport has universal characteristics at the Mott transition, on which we focus in the following. The conductance can be obtained from the zero frequency limit of

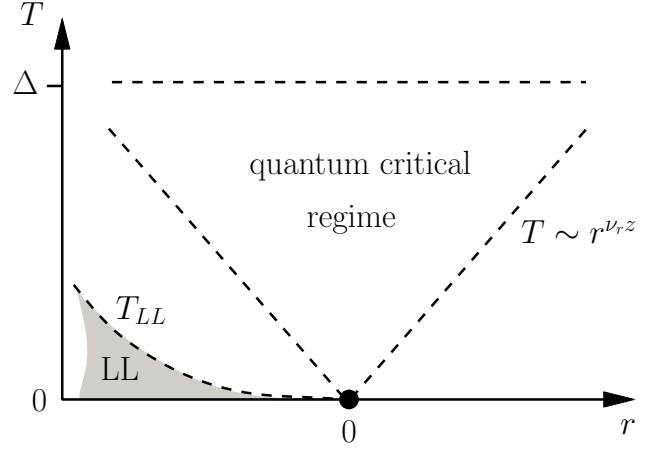


FIG. 1: Phase diagram of the CI transition for temperatures smaller than the gap Δ , see text. A quantum phase transition with exponents $\nu_r = 1/2$ and $z = 2$ separates the commensurate, $r > 0$, and the incommensurate, $r < 0$, phases. The CI Hamiltonian (2.13) controls the vicinity of the quantum critical point. The quantum critical regime occurs within a cone $T \sim |r|^{\nu_r z} = |r|$.

the conductivity,²³

$$G = \lim_{\omega \rightarrow 0} \sigma(x, x'; \omega), \quad (2.16)$$

at fixed positions x and x' . The conductivity $\sigma(x, x'; \omega)$ describes the linear response of the charge current at position x upon applying an external²⁴ electric field $\mathcal{E}(x', \omega)$ at position x' with frequency ω

$$\langle J(x, \omega) \rangle = \int dx' \sigma(x, x'; \omega) \mathcal{E}(x', \omega). \quad (2.17)$$

The conductivity is derived with the help of the Kubo formula that relates σ to the charge current autocorrelation function

$$\sigma(x, x'; \omega) = \frac{\mathcal{K}_{x, x'; \omega}^{\text{ret}} - \mathcal{K}_{x, x'; \omega=0}^{\text{ret}}}{i\omega}, \quad (2.18)$$

where the retarded function is defined by

$$\mathcal{K}_{x, x'; \omega}^{\text{ret}} = i \int dt e^{i\omega t} \langle [J(x, t), J(x', 0)] \rangle. \quad (2.19)$$

The subtraction of the $\omega = 0$ mode in (2.18) ensures gauge invariance. In the following, it will be convenient to obtain the retarded response function from the temperature correlation function

$$\mathcal{K}_{x, x'; \Omega_n} = \int_0^{1/T} d\tau e^{i\Omega_n \tau} \langle T_\tau J(x, \tau) J(x', 0) \rangle \quad (2.20)$$

by the analytic continuation from the upper half-plane, $\mathcal{K}_{x, x'; \omega}^{\text{ret}} = \mathcal{K}_{x, x'; \Omega_n} |_{i\Omega_n \rightarrow \omega + i0}$, where $\Omega_n = 2\pi nT$ is the bosonic Matsubara frequency.

D. Critical conductance of the homogeneous system

Consider first the uniform system close to the metal-insulator transition. At the criticality, the transport is determined by the free nonrelativistic c -fermions, i.e., by the Hamiltonian (2.13). The resulting conductance

$$G^{(\text{hom})} = \frac{2e_{\text{CI}}^2}{h} f(r/T) = \frac{1}{2} G_0 f(r/T) \quad (2.21)$$

is simply the conductance quantum $2e_{\text{CI}}^2/h$ for the effective fermions with charge (1.4), times the occupation factor that is given by the Fermi distribution (1.3).

The critical conductance is universal and its temperature dependence is controlled by a Fermi function (1.3). The non-universal corrections arising from the residual interaction (2.14) vanish with the distance to the quantum critical point as the interaction γ is an irrelevant perturbation. In particular, in the limit of low temperatures the conductance at criticality, $r = 0$, approaches the value

$$G^{(\text{hom})} \Big|_{r=0, T \rightarrow 0} = \frac{1}{4} G_0. \quad (2.22)$$

At zero temperature the conductance $G^{(\text{hom})} \Big|_{T=0, r \rightarrow 0_+} \equiv 0$ in the insulating phase, while in the metallic phase $G^{(\text{hom})} \Big|_{T=0, r \rightarrow 0_-} = \frac{1}{2} G_0$, thus the conductance exhibits a jump across the transition of the height

$$G^{(\text{hom})} \Big|_{T=0, r \rightarrow 0_-} - G^{(\text{hom})} \Big|_{T=0, r \rightarrow 0_+} = \frac{1}{2} G_0. \quad (2.23)$$

The factor $\frac{1}{2}$ originates from the fractional nature of the charge carried by the critical fermionic degrees of freedom, $e_{\text{CI}} = e/\sqrt{2}$. As was pointed out in Ref. 25, the conductance jump across the transition (2.23) in fact corresponds to a full conductance quantum but with fractional charge, $G_0/2 = 2e_{\text{CI}}^2/h$.

In the following section the modifications to the critical conductance (2.21) due to the presence of leads attached to the Mott wire are discussed.

III. CRITICAL CONDUCTANCE IN THE PRESENCE OF LEADS

In a two-terminal conductance measurement the critical Mott wire will be connected to leads. In the presence of leads the conductance will differ from the expression (2.21) for the homogeneous system. We assume here that the leads contain Luttinger liquids characterized by the Luttinger parameter K_L . Here we argue that the critical conductance is that of the homogeneous case, Eq. (2.21), *only* if the Luttinger parameter K_L has the Luther-Emery value $K_L = 1/2$. Note that this value of K_L corresponds to *strong* interaction between the original electrons in the leads. If K_L differs from $\frac{1}{2}$, the universal

properties of the critical conductance are modified. Below we develop the perturbation theory in the deviation from the Luther-Emery point, and evaluate the critical conductance in the first order in $K_L - \frac{1}{2}$.

A. Leads with Luttinger parameter $K_L = \frac{1}{2}$

The Ψ fermions entering the Thirring model (2.7) are the appropriate degrees of freedom describing the Mott transition as the interaction, g_2 and g_4 , among them is irrelevant. In the following we will also adopt a description of the leads, where the Mott gap is absent, $\Delta = 0$, in terms of the same Ψ -fermions. The advantage of such a description is that the Mott region of the wire can be incorporated into an effective scattering approach for the Ψ fermions which is outlined in the following. The caveat is that, unfortunately, these effective fermions will in general, i.e. for $K_L \neq \frac{1}{2}$, interact within the leads. This is what makes this problem difficult, as one has to solve the strongly interacting fermionic problem which also lacks translation invariance. The influence of the interaction within the leads is considered in Section III B perturbatively.

Mori *et al.* in Ref. 7 considered a very similar setup as we do here. They also calculated the current-current correlation function with the help of the Ψ fermions at the Luther-Emery point but only for the uniform system, where the Mott gap extends over the full wire. They proceeded by using the expression for the homogeneous case to derive the conductance in the presence of the leads where the original electrons do not interact. We think that the last step has led them to the erroneous result for the temperature dependence of the critical conductance. We will further elaborate on the difference between the treatment of Mori *et al.* and ours in Section IV.

1. Scattering states

Let us consider the situation where the Luttinger parameter of the leads $K_L = \frac{1}{2}$, corresponding to $g_2 \equiv 0$ in the Hamiltonian (2.7). Here we also set $g_4 = 0$. The absence of interactions allows us to describe the wire in terms of a simple 1D scattering problem. The leads can then be characterized by the states of the Ψ fermions that scatter off the Mott region. The crucial point is that the latter will be treated as an effective point scatterer. This is a correct approximation for the dc Landauer transport, and physically it means that we attach infinitely long leads to the Mott region.

The scattering wave incident from the left has the stan-

dard form

$$\psi_{\epsilon,+}(x) = \frac{1}{\sqrt{2\pi v}} \begin{cases} e^{i\epsilon x/v} \begin{pmatrix} 1 \\ 0 \end{pmatrix} + e^{-i\epsilon x/v} r_L(\epsilon) \begin{pmatrix} 0 \\ 1 \end{pmatrix}, & x < 0 \\ e^{i\epsilon x/v} t_L(\epsilon) \begin{pmatrix} 1 \\ 0 \end{pmatrix}, & x > 0. \end{cases} \quad (3.1a)$$

The energy ϵ is measured here (and everywhere below) with respect to the Fermi level. The phase velocity in the R- and L- moving states (upper and lower spinor components) equals $\pm v$ correspondingly. The wave incident from the right reads

$$\psi_{\epsilon,-}(x) = \frac{1}{\sqrt{2\pi v}} \begin{cases} e^{-i\epsilon x/v} t_R(\epsilon) \begin{pmatrix} 0 \\ 1 \end{pmatrix}, & x < 0 \\ e^{-i\epsilon x/v} \begin{pmatrix} 0 \\ 1 \end{pmatrix} + e^{i\epsilon x/v} r_R(\epsilon) \begin{pmatrix} 1 \\ 0 \end{pmatrix}, & x > 0. \end{cases} \quad (3.1b)$$

The transmission and reflection coefficients are components of the scattering S-matrix,

$$\mathbf{S}(\epsilon) = \begin{pmatrix} t_L(\epsilon) & r_R(\epsilon) \\ r_L(\epsilon) & t_R(\epsilon) \end{pmatrix}, \quad (3.2)$$

which is unitary, $\mathbf{S}^\dagger \mathbf{S} = \mathbf{1}$. The unitarity of the S-matrix ensures that it has only three independent parameters, which can be chosen in the form

$$t_L = t_R = t e^{i\phi_t}, \quad r_L = -r e^{i\phi_-}, \quad r_R = r e^{i\phi_+} \quad (3.3)$$

with $\phi_t = (\phi_+ + \phi_-)/2$, and positive r and t , $r^2 + t^2 = 1$. The relation $t_L = t_R$ is a consequence of the time-reversal symmetry.

The presence of the Mott gap at the center of the wire makes the transmission and the reflection coefficients strongly energy-dependent: The propagation is blocked for the fermionic states with energies within the gap, $\epsilon < r$. These states therefore have zero transmission coefficient as we assume the Mott gapped region of the wire to be sufficiently long such that the tunneling across it can be neglected. On the other hand, the fermionic states with energies above the gap, $\epsilon > r$, are able to traverse the Mott region. We will assume that the leads are attached to the Mott-gapped region of the wire in the adiabatic fashion (i.e. $V_{\text{Uml}} = V_{\text{Uml}}(x)$ is a smooth function), such that the backscattering of particles moving above the gap can be neglected. The tuning parameter, r , of the transition thus divides the fermionic scattering states into the propagating waves with unit transmission for energies $\epsilon > r$, and into the standing waves for energies $\epsilon < r$. As a result, we model the Mott region of the wire by utilizing simple unit step-function transmission and reflection amplitudes

$$t(\epsilon) = \Theta(\epsilon - r), \quad r(\epsilon) = \Theta(r - \epsilon). \quad (3.4)$$

Summarizing,

$$\mathbf{S}(\epsilon) = \begin{pmatrix} \Theta(\epsilon - r) e^{i\phi_t(\epsilon)} & \Theta(r - \epsilon) e^{i\phi_+(\epsilon)} \\ -\Theta(r - \epsilon) e^{i\phi_-(\epsilon)} & \Theta(\epsilon - r) e^{i\phi_t(\epsilon)} \end{pmatrix}. \quad (3.5)$$

The scattering phases $\phi_\pm(\epsilon)$ are accumulated while traversing or reflecting from the Mott barrier. The barrier shape is encoded in their smooth energy dependencies,

$$\phi_\pm(\epsilon) \simeq \phi_\pm^0 + \ell_\pm \epsilon / v, \quad (3.6)$$

The scattering lengths ℓ_\pm are a measure of the effective length of the region of the wire where the Mott gap is present.

2. Green's Function

The single-particle *Green's function* in the Matsubara representation is a 2×2 matrix in the spinor space [$a, b = 1, 2$ are the spinor components of the wave functions (3.1)]

$$\mathcal{G}_{x,x';\tau}^{ab} = -\langle T_\tau \psi^a(x, \tau) \psi^{\dagger b}(x', 0) \rangle. \quad (3.7a)$$

In what follows we will be using its Lehmann representation

$$\mathcal{G}_{x,x';\omega_n} = \int d\epsilon \frac{\mathbf{A}_{x,x';\epsilon}}{i\omega_n - \epsilon}, \quad (3.7b)$$

$$\text{where } \mathbf{A}_{x,x';\epsilon}^{ab} = \sum_{\sigma=\pm} \psi_{\epsilon,\sigma}^a(x) \psi_{\epsilon,\sigma}^{\dagger b}(x'), \quad (3.7c)$$

and $\omega_n = \pi(2n+1)T$ is a fermionic Matsubara frequency.

As we show now, the Green's function (3.7) has qualitatively different properties when its arguments x and x' are located on the same and on the opposite sides of the impermeable potential barrier. Introducing the labels

$$s = \text{sign } x \quad \text{and} \quad s' = \text{sign } x', \quad (3.8)$$

one finds:

$s \neq s'$:

$$\mathbf{A}_{x,x';\epsilon} = \nu \Theta_{\epsilon-r} \begin{pmatrix} e^{i\epsilon(x-x')/v + is\phi_t(\epsilon)} & 0 \\ 0 & e^{-i\epsilon(x-x')/v - is\phi_t(\epsilon)} \end{pmatrix} \quad (3.9a)$$

$s = s'$:

$$\begin{aligned} \mathbf{A}_{x,x';\epsilon} = & \nu \begin{pmatrix} e^{i\epsilon(x-x')/v} & 0 \\ 0 & e^{-i\epsilon(x-x')/v} \end{pmatrix} \\ & + \nu s \Theta_{r-\epsilon} \begin{pmatrix} 0 & e^{i\epsilon(x+x')/v + is\phi_s(\epsilon)} \\ e^{-i\epsilon(x+x')/v - is\phi_s(\epsilon)} & 0 \end{pmatrix}. \end{aligned} \quad (3.9b)$$

The spectral function (3.9a), as well as the first term in the spectral function (3.9b) become translation-invariant in the limit $|x - x'| \rightarrow \infty$, since they both depend only on the coordinate difference $x - x'$. They originate from the propagating states and from the corresponding co-moving parts of the standing waves. The second term in Eq. (3.9b) is due to the counter-moving parts of the standing waves and comes only from the states with energies below the barrier, $\epsilon < r$. It lacks translational invariance, and is affected by the barrier shape through the energy-dependent reflection phase shifts ϕ_\pm .

3. Polarization operator

A basic ingredient in the following calculation is the polarization operator that is a convolution of the temperature Green functions (3.7),

$$\Pi_{x,x';\Omega_n}^{ij} = -T \sum_{\omega_n} \text{tr} \{ \tau^i \mathcal{G}(x, x'; \omega_n + \Omega_n) \tau^j \mathcal{G}(x', x; \omega_n) \} \quad (3.10)$$

where $i, j = 0, 1$ and

$$\tau^i = \begin{pmatrix} 1 & 0 \\ 0 & \beta^i \end{pmatrix}, \quad \text{with} \quad \beta^i = \begin{cases} +1, & i = 0; \\ -1, & i = 1. \end{cases} \quad (3.11)$$

The polarization matrix $\Pi_{x,x';\Omega_n}^{ij}$ depends on the bosonic Matsubara frequency $\Omega_n = 2\pi nT$. A detailed calculation of the above expression can be found in the Appendix A. In the dc limit ($i\Omega_n \rightarrow \omega + i0$, $\omega \rightarrow 0$) it reduces to

$$\begin{aligned} \Pi_{x,x';\Omega_n}^{ij} &= \Pi_{x,x';\Omega_n}^{(0)ij} + [f(r/T) - 1] \\ &\times \left\{ \frac{1 - ss'}{2} \Pi_{x,x';\Omega_n}^{(0)ij} - \beta^j \frac{1 + ss'}{2} \Pi_{x,-x';\Omega_n}^{(0)ij} \right\}, \end{aligned} \quad (3.12)$$

where f is the Fermi function (1.3), and we used the abbreviation (3.8). The polarization operator matrix in the absence of the Mott barrier is

$$\Pi_{x,x';\Omega_n}^{(0)ij} = 2\nu \delta_{ij} \delta(x - x') + \bar{\Pi}_{x,x';\Omega_n}^{ij}, \quad (3.13)$$

$$\begin{aligned} \bar{\Pi}_{x,x';\Omega_n} &= -2\pi\nu^2 e^{-|\Omega_n||x-x'|/v} \\ &\times \begin{pmatrix} |\Omega_n| & \Omega_n \text{sign}(x - x') \\ \Omega_n \text{sign}(x - x') & |\Omega_n| \end{pmatrix}, \end{aligned} \quad (3.14)$$

with the density of states (2.10). The rows and columns of the matrix (3.14) are numbered by the indices $i, j = 0, 1$, such that $\bar{\Pi}^{00}$ corresponds to the upper left corner. The corrections to the result (3.12) are subleading in powers of frequency Ω_n , see Appendix A for details.

Let us discuss the meaning of the expression (3.12). The trivial observation is that, in the absence of the barrier, $f = 1$, and $\Pi \equiv \Pi^{(0)}$ becomes translation invariant. In the opposite case of an infinitely high barrier, $f = 0$, and $\Pi_{x,x';\Omega_n}^{ij} \equiv 0$ identically vanishes when the points x and x' are on the opposite sides of the barrier (no transmission). We now consider the polarization operator when x and x' are on the same side, $\Pi_{x,x';\Omega_n}^{ij} = \Pi_{x,x';\Omega_n}^{(0)ij} + \beta^j \Pi_{x,-x';\Omega_n}^{(0)ij}$. This expression has a static part (that remains finite in the limit $\Omega_n \rightarrow 0$), and the dynamic part $\propto \Omega_n$. The static part of the compressibility $\Pi_{x,x';\Omega_n=0}^{00} = 2\nu \delta(x - x')$ is not affected by the barrier at all (this in fact is true for any value of f), as the density of states in the leads is independent of the barrier. The dynamic part is more interesting. For $f = 0$, it is given by $\bar{\Pi}_{x,x';\Omega_n}^{ij} + \beta^j \bar{\Pi}_{x,-x';\Omega_n}^{ij}$. This expression can be understood by looking at the dynamic part of the current-current correlator, corresponding to $i = j = 1$. After the analytic continuation it behaves $\propto \omega e^{i\omega x/v} \sin(\omega x'/v)$. Therefore, the conductivity (2.18)

vanishes as $\sin(\omega x'/v)$ in the dc limit: Given enough time, the system finds out about the barrier. For finite f , the part of the expression (3.12) responsible for the transmission of the particles is proportional to $f(r/T)$.

Technically, the presence of the barrier leads to an additional term in the expression (3.12) that is multiplied by the factor $f(r/T) - 1$. This term can be further simplified by noting that, in the dc limit, the point-scatterer approximation for the Mott region allows us to substitute $|x + x'| = |x| + |x'|$ for $s = s'$, and $|x - x'| = |x| + |x'|$ for $s \neq s'$, yielding

$$\Pi_{x,x';\Omega_n}^{(0)ij} = \bar{\Pi}_{x,0;\Omega_n}^{ij} e^{-|\Omega_n x'|/v}, \quad s \neq s', \quad (3.15)$$

$$\Pi_{x,-x';\Omega_n}^{(0)ij} = \bar{\Pi}_{x,0;\Omega_n}^{ij} e^{-|\Omega_n x'|/v}, \quad s = s'. \quad (3.16)$$

Using the above simplification the expression Eq. (3.12) can be cast into a form characteristic for a scattering problem,

$$\Pi_{x,x';\Omega_n} = \Pi_{x,x';\Omega_n}^{(0)} + \bar{\Pi}_{x,0;\Omega_n} \hat{\mathfrak{T}} \bar{\Pi}_{0,x';\Omega_n}. \quad (3.17)$$

In the limit of small Ω_n (in the sense of analytic continuation $i\Omega_n \rightarrow \omega \rightarrow 0$ specified above), the scattering $\hat{\mathfrak{T}}$ -matrix is given by

$$\hat{\mathfrak{T}} = \begin{pmatrix} 0 & 0 \\ 0 & \mathfrak{T} \end{pmatrix}, \quad \mathfrak{T} = \frac{1 - f(r/T)}{2\pi\nu^2 |\Omega_n|}. \quad (3.18)$$

4. Critical conductance with leads at the Luther-Emery point $K_L = \frac{1}{2}$

From the evaluated polarization matrix (3.17) we can derive the conductance in the presence of leads that have a Luttinger parameter of the Luther-Emery value $K_L = \frac{1}{2}$. The current autocorrelator (2.20) is then given by

$$\mathcal{K}_{x,x';\Omega_n}^{\text{LE}} = 2e_{\text{CI}}^2 v^2 \Pi_{x,x';\Omega_n}^{11}. \quad (3.19)$$

The conductance (2.16) follows from the Kubo formula (2.18),

$$G_{\text{LE}} = \frac{1}{2} G_0 f(r/T), \quad (3.20)$$

with the conductance quantum $G_0 = 2e^2/h$. We thus reproduce the critical conductance of the homogeneous system (2.21). Below, we show how the critical properties of the conductance are modified in first order in the deviation $K_L - \frac{1}{2}$.

B. Critical conductance: Perturbation theory around the Luther-Emery point

Here we evaluate the correction to the conductance arising from the deviation of the Luttinger parameter in the leads from its Luther-Emery value $K_L = \frac{1}{2}$. The

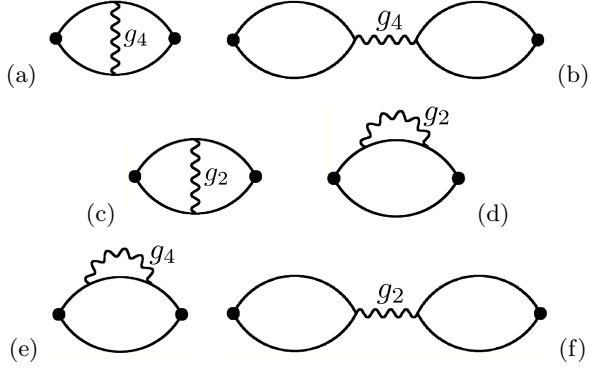


FIG. 2: First order corrections to the current autocorrelator. The straight line represent fermionic Ψ propagators, the wiggled line is the interaction and the dot is the current vertex $\sqrt{2}e_{\text{CI}}v\sigma^3$.

deviation from $K_L = \frac{1}{2}$ implies according to Eq. (2.9) a finite g_2 interaction between the scattering Ψ fermions. In the following we calculate the conductance up to the first order in the interactions g_2 and g_4 . As in the first order the g_4 interaction only modifies the velocity, it is expected that it does not enter the conductance correction. The verification of this expectation serves as a check of our calculation and is actually the only reason to introduce at all the redundant g_4 interaction in the mapping (2.8) and (2.9).

There are various contributions to conductance arising from finite g_2 and g_4 . First of all, these interactions modify the expression of the charge current velocity v_J , see Eq. (2.12). As a consequence, the conductance obtains the modification,

$$\delta G^A / G_{\text{LE}} = 2(g_4\nu - g_2\nu). \quad (3.21)$$

In addition, there are in total six first order diagrams that contribute to the current autocorrelator, see Fig. 2. Diagrams (a) and (b) cancel each other exactly due to the Fermi statistics. Diagram (c) does not modify the conductance because its contribution to $\sigma(x, x'; \omega)$ vanishes in the low frequency limit. In the absence of the barrier this is self-evident, as the small frequencies correspond to small incoming momenta that cannot change an R-mover into a L-mover. In the presence of the barrier this argument essentially goes through, since only the propagating parts (3.9a) of the Green's functions contribute; the latter have the same diagonal form as in the translation-invariant problem. Diagram (d) corresponds to the conductance correction coming from fermion scattering off a Friedel oscillation;^{26,27,28} we will see that in our case this contribution is absent. The only modifications to the conductance arise from the self-energy diagram (e) and from the random-phase approximation (RPA) diagram (f). They are discussed in detail below.

1. Scattering off Friedel oscillations: Diagram (d)

The self-energy correction in diagram (d) embodies the scattering off a Friedel oscillation. In the general case of a semitransparent barrier, this process leads to a logarithmic renormalization of the scattering coefficients and of the conductance.^{26,27,28} However, the S-matrix in our case has a very specific energy dependence (3.5) as the transmission at a given energy is either zero or unity. In such a situation the renormalization e.g. of the transmission coefficient vanishes as it is proportional to the product of transmission and reflection coefficients at a given energy. As a consequence, diagram (d) does not contribute to the conductance here.

The fact that there is no contribution from the Friedel oscillation in the first order in g_2 can be understood already from the following simple argument. Consider the propagating state, for which the transmission is unity in the absence of interactions between fermions. Due to the interaction g_2 with the counterpropagating states, the reflection amplitude will appear, being proportional to g_2 , thus the reflection probability is $\mathcal{O}(g_2^2)$. This means that the transmission amplitude (and the probability) is of the form $1 - \mathcal{O}(g_2^2)$, i.e. the correction to the transmission (and hence, to the conductance) vanishes to the first order in g_2 .

2. Density of states renormalization: Diagram (e)

The other fermionic self-energy that appears in diagram (e) in Fig. 2 arises from the g_4 interaction. The left and right moving fermions interact only among themselves via g_4 which ensures that the resulting self-energy is translationally invariant,

$$\widehat{\Sigma}^{(e)}(x, x') = -\frac{g_4(x, x')}{2\pi i(x - x')} \sigma^3, \quad (3.22)$$

as $g_4(x, x') = g_4(x - x')$. This self-energy causes a perturbative correction to the velocity of the scattering particles. This is seen from the analysis of the Schrödinger equation for the scattering states,

$$-iv\sigma^3\partial_x\psi_\epsilon(x) + \int dx' \widehat{\Sigma}^{(e)}(x, x')\psi_\epsilon(x') = \epsilon\psi_\epsilon(x). \quad (3.23)$$

The Schrödinger equation can be solved perturbatively with the help of the Wentzel-Kramers-Brillouin ansatz

$$\psi_\epsilon(x) \propto \exp\left(i\sigma^3 \int^x dy \varphi(y)\right) \quad (3.24)$$

where in zeroth order $\varphi^{(0)} = \epsilon/v$. The first order correction to the eikonal phase is determined by

$$\varphi^{(1)}(x) = \int dx' \frac{g_4(x, x')}{2\pi v i(x - x')} e^{i\epsilon(x' - x)/v}. \quad (3.25)$$

In particular, the energy derivative of the eikonal phase up to first order is given by

$$\frac{\partial \varphi}{\partial \epsilon} = \frac{1 - \nu g_4}{v} \quad (3.26)$$

where $g_4 = \int dx' g_4(x - x') e^{i\epsilon(x' - x)/v}$ is the Fourier transform of the g_4 interaction at small wavevector ϵ/v . This is equivalent to the renormalization of the velocity $v \rightarrow v + \delta v$, where $\delta v/v = g_4 \nu$.

The velocity renormalization enters the normalization of the scattering states (3.1a) and (3.1b) and thus contributes to the conductivity by changing the density of states, $\nu \rightarrow \nu(1 - \nu g_4)$. The density of states on the other hand enters the polarization matrix (3.17) which finally leads to the change in the conductance

$$\delta G^{(e)}/G_{LE} = -2g_4 \nu \quad (3.27)$$

attributed to diagram (e).

3. Random-phase approximation contribution: Diagram (f)

The remaining RPA diagram (f) in Fig. 2 can be reduced to the spatial convolutions of the two components of the polarization matrix (3.10). The resulting correction to the current autocorrelator (2.20) reads

$$\begin{aligned} \delta \mathcal{K}^{(f)}(x, x'; \Omega_n) = & \quad (3.28) \\ -g_2 e_{CI}^2 v^2 \int dx_1 & [\Pi_{x,x_1;\Omega_n}^{10} \Pi_{x_1,x';\Omega_n}^{01} - \Pi_{x,x_1;\Omega_n}^{11} \Pi_{x_1,x';\Omega_n}^{11}] \end{aligned}$$

As we are only interested in the behavior at small frequency Ω_n , we can use the simplified expressions (3.17) for the polarization operators. The integral over x_1 can then be performed with the help of the convolution (no summation over index i implied)

$$\begin{aligned} & \int dx_1 \bar{\Pi}_{x,x_1;\Omega_n}^{1i} \bar{\Pi}_{x_1,x';\Omega_n}^{i1} \\ &= \nu \bar{\Pi}_{x,x';\Omega_n}^{11} \left(\beta_i - \frac{|\Omega_n|}{v} |x - x'| \right) \end{aligned} \quad (3.29)$$

where β_i was defined in Eq. (3.11) and $\bar{\Pi}^{ij}$ in Eq. (3.14). After the evaluation of the x_1 integral, we obtain for the RPA contribution

$$\begin{aligned} \delta \mathcal{K}^{(f)}(x, x'; \Omega_n) = & -2g_2 \nu e_{CI}^2 v^2 [-2\nu \delta(x - x') \\ & - \bar{\Pi}_{x,x';\Omega_n}^{11} + \bar{\Pi}_{x,0;\Omega_n}^{11} \mathfrak{T} \bar{\Pi}_{0,0;\Omega_n}^{11} \mathfrak{T} \bar{\Pi}_{0,x';\Omega_n}^{11}] \end{aligned} \quad (3.30)$$

The presence of the product of bosonic T-matrices, \mathfrak{T} , see Eq. (3.18), leads to the correction to conductance that contains an additional Fermi function,

$$\delta G^{(f)}/G_{LE} = \nu g_2 [2 - f(r/T)]. \quad (3.31)$$

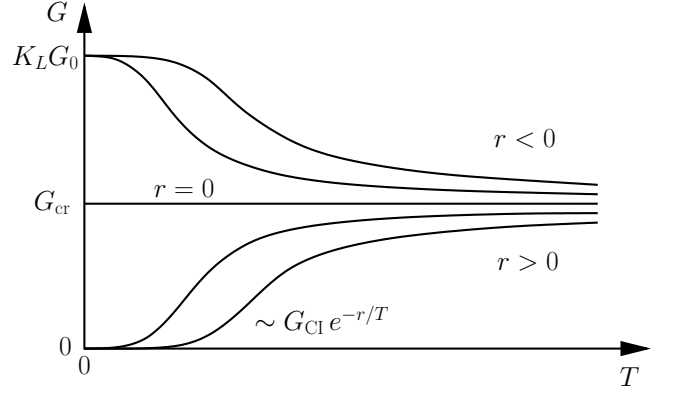


FIG. 3: Temperature dependence of two-terminal conductance close to the Mott transition for different values of the tuning parameter r . On the metallic side, $r < 0$, at $T = 0$ the conductance is determined by the Luttinger parameter of the leads, K_L ; $G_0 = 2e^2/h$ is the conductance quantum. In the insulating phase, $r > 0$, at lowest temperature the conductance is thermally activated with a universal exponential prefactor involving the fractional charge, $e_{CI} = e/\sqrt{2}$, of the critical degrees of freedom, $G_{CI} = 2e_{CI}^2/h$. In the quantum critical regime, $|r| < T$, of the phase diagram, see Fig. 1, the conductance is determined by its critical value, G_{cr} , see Eq. (1.5), that depends both on the Luttinger parameter, K_L , and on the fractional charge, e_{CI} .

4. Full perturbative correction

Collecting all the perturbative contributions to conductance, (3.21), (3.27) and (3.31), we obtain the following for the first order correction in the parameter $K_L - \frac{1}{2}$,

$$\delta G/G_0 = -\frac{\nu g_2}{2} f^2(r/T) = (K_L - \frac{1}{2}) f^2(r/T), \quad (3.32)$$

where we used the identification $\nu g_2 = 1 - 2K_L$ valid to the first order in g_2 , cf. Eq. (2.9). As expected, the first order correction to conductance is independent of g_4 . Note that the correction starts with the square of the Fermi function whose origin can be traced back to the RPA diagram (f) in Fig. 2. Adding to this the zeroth order contribution (3.20) we finally obtain the result announced in Eq. (1.2).

IV. SUMMARY AND DISCUSSION

In the present work we considered the finite-temperature dc conductance close to the commensurate-incommensurate Mott transition in a one-dimensional wire as a function of the tuning parameter, r , of the transition. For a homogeneous system in the absence of leads the result is universal and is given by Eq. (2.21). It is determined by the critical degrees of freedom of the transition — the fermionic charge carriers that have a fractional charge $e_{CI} = e/\sqrt{2}$, — and the temperature dependence is simply a Fermi function.

Furthermore, we addressed the question on how the conductance is modified when the leads are attached to the Mott wire. The result is summarized in Fig. 3. In the incommensurate phase, $r < 0$, when the system is a metal, the dc conductance at zero temperature does not contain any information about the universal signatures of the Mott transition because it is solely determined by the compressibility of the electron liquid in the leads, i.e., by the Luttinger parameter K_L in agreement with Refs. 6 and 7. However, in the insulating phase, $r > 0$, we found evidence that the critical degrees of freedom of the quantum phase transition become manifest in the dc transport. In particular, in the lowest order in the fugacity $e^{-r/T}$, the conductance is independent of the properties of the leads, K_L , while the exponential prefactor is determined by the universal characteristic of the Mott transition as it is given by an effective conductance quantum of the fractional charge carriers, $G_{\text{CI}} = 2e_{\text{CI}}^2/h$. The conductance in this regime originates from thermal activation of solitonic excitations that travel ballistically across the Mott-gapped region of the wire. Finally, in the quantum critical regime, $|r| < T$, of the phase diagram in Fig. 1 the conductance is dominated by its critical value (1.5) that depends on the Luttinger parameter of the leads, K_L , as well as on the fractional charge e_{CI} .

Our main finding is that the dc transport shows signatures of charge fractionalization (1.4) in the Mott wire. The underlying reason is that the electrons, irrespective of their interactions in the leads, must “transform” into Mott solitons with charge (1.4) in order to overcome the Mott barrier Δ . The fractional charge can in principle be detected with the help of the finite temperature behavior of the critical two-terminal conductance of a Mott wire. We contrast this fractionalization with that in a Luttinger-liquid wire, where only the forward scattering is included;¹ there, the phenomenon of fractionalization is not manifest in the dc conductance.^{3,4,5}

The regime discussed above is restricted to the immediate vicinity of the quantum critical point of Fig. 1, i.e. to the temperatures and to the tuning parameter much smaller than the Mott gap: $|r|, T \ll \Delta$. In particular, we neglected corrections arising from the thermal activation of particles in the other Mott band which are exponentially small in $e^{-(2\Delta-r)/T}$. Furthermore, we disregarded effects of tunneling of solitons through the Mott barrier, which gives rise to a finite conductance in the insulating regime of the form $\delta G \sim e^{-S}$, where $S \propto rL/v$ with the length of the barrier L and the velocity of solitons v . The approximation of neglecting this tunneling correction breaks down at sufficiently low temperatures when the length L becomes comparable to the thermal wavelength $\xi_T = v/T$.

We arrived at our conclusions by performing a controlled perturbative expansion around the special value $K_L = 1/2$ of the Luttinger parameter in the leads. At this specific Luther-Emery value, the solitonic excitations are free, and the problem of the Mott wire with leads reduces to a 1D scattering problem as described in Section

III A. For K_L different from the Luther-Emery value, the interaction between the scattering states in the leads yields the result (1.2).

Our conclusions concerning the temperature dependence of the critical conductance differ from the results of the work of Mori *et al.*⁷ There, a similar setup was considered, and the current autocorrelation function was also calculated in terms of the critical degrees of freedom of the Mott transition. However, the current correlator was only considered for a homogeneous system when the Mott gap extends across the full wire length resulting in a translationally invariant expression. The result was then used to match the current autocorrelator within the Mott wire with the one of the Fermi liquid leads in order to derive the conductance. We believe, however, that the use of the current autocorrelator for the homogeneous Mott wire is inconsistent with the matching conditions applied in Ref. 7, which explicitly break translational invariance. Instead of using the homogeneous current autocorrelation function one may consider the result (3.17) for the case of a gapped region inside the wire as a starting point for a matching procedure. Preliminary considerations along these lines have led us to the conjecture described below.

Let us speculate about the functional form of dc conductance beyond the leading $K_L - \frac{1}{2}$ correction. We conjecture that, in the limit $|r|, T \ll \Delta$ and $T \gg v/L$, the corresponding resistance is a sum of the two contributions

$$R = R_L + R_M \quad \text{with} \quad (4.1)$$

$$R_L = \frac{1}{K_L} \frac{h}{2e^2}, \quad \text{and} \quad R_M = \frac{h}{2e_{\text{CI}}^2} \frac{1 - f(r/T)}{f(r/T)},$$

where $e_{\text{CI}} = e/\sqrt{2}$ and f is the Fermi function (1.3). The resistance R_L is attributed to the leads and can be interpreted as a contact resistance. In particular, only R_L depends on the Luttinger parameter within the leads, K_L . The contribution R_M has the form of a four-terminal resistance with an effective transmission given by the Fermi function, $f(r/T)$. It originates from the critical Mott part of the wire and involves the charge quantum of the critical degrees of freedom, e_{CI} . The expression (4.1) reproduces the known limits. In the incommensurate phase, $r < 0$, at $T = 0$ the resistance reduces to the contact resistance $R = R_L$. In the insulating state, $r > 0$, at lowest temperature the resistance is dominated by the contribution of the Mott region R_M and becomes independent of the lead properties. Expanding (4.1) in $K_L - \frac{1}{2}$ one also reproduces our hard-to-guess perturbative result (1.2).

The Mott region in a quantum wire may be realized by employing an external periodic potential created by gating,²⁹ or an acoustic field.³⁰

Our approach applies also to the problem of drag between two quantum wires. At equal electron densities, the inter-wire interaction locks the charges in both wires such that the drag resistance at $T = 0$ is infinite in the

commensurate state. This system bears resemblance to the Mott insulator: if opposite biases are applied to the two wires, there is no current at $T = 0$.^{31,32} Density imbalance drives the system into an incommensurate phase, for which one recovers the ballistic conductance for each of the wires; drag is absent at $T = 0$. The problem of a finite- T drag resistance may be mapped onto that of the critical conductance in a Mott wire. Technically, such a mapping is established by introducing the even and odd modes, $\rho_{\pm} = (\rho_1 \pm \rho_2)/\sqrt{2}$, where $\rho_{1,2}(x)$ are the electron densities in the two wires. The dynamics of the odd mode is described by the sine-Gordon model (2.1), while the even mode is a conventional Luttinger liquid. The drag resistance is determined by the conductance in the odd sector. The present analysis of the critical behavior of the transport at the commensurate-incommensurate transition is fully applicable for the evaluation of the drag resistance.

Acknowledgments

M.G. was supported by SFB 608 of the DFG. D.N. and L.G. were supported by NSF grants DMR 02-37296 and DMR 04-39026. A.S. acknowledges financial support by the Israel Science Foundation, administered by the Israeli Academy of Sciences.

APPENDIX A: POLARIZATION OPERATOR IN THE COORDINATE-FREQUENCY REPRESENTATION

We present a detailed calculation of the polarization operators (3.10). After performing the sum over fermionic Matsubara frequencies we obtain

$$\Pi_{x,x';\Omega_n}^{ij} = \int d\epsilon d\epsilon' \frac{f(\epsilon) - f(\epsilon')}{i\Omega_n - (\epsilon - \epsilon')} \text{tr} \{ \tau^i \mathbf{A}_{x,x';\epsilon} \tau^j \mathbf{A}_{x',x;\epsilon'} \} \quad (\text{A1})$$

with the spectral function \mathbf{A} given in (3.9). In this section, we use a temperature dependent definition of the Fermi function, $f(\omega) = 1/(e^{\omega/T} + 1)$. As a first step we evaluate the trace. We will use the abbreviations (3.8). Consider first a situation with $s \neq s'$, i.e. with x and x' on opposite sides of the barrier.

$$s \neq s' : \quad \text{tr} \{ \tau^i \mathbf{A}_{x,x';\epsilon} \tau^j \mathbf{A}_{x',x;\epsilon'} \} = \nu^2 \Theta_{\epsilon-r} \Theta_{\epsilon'-r} \mathcal{A}_{\epsilon,\epsilon'}^{ij}(x - x' + s\ell_t). \quad (\text{A2})$$

Here

$$\mathcal{A}_{\epsilon,\epsilon'}^{ij}(x) = e^{i(\epsilon-\epsilon')x/v} + \beta^i \beta^j e^{-i(\epsilon-\epsilon')x/v}, \quad (\text{A3})$$

where the β^i were defined in (3.11); and we made use of the approximations (3.6) for the phase shifts with $\ell_t = (\ell_+ + \ell_-)/2$. The case $s = s'$ is done explicitly

[in Eq. (A4) set $v = 1$ for brevity]:

$$\begin{aligned} s = s' : \quad & \text{tr} \{ \tau^i \mathbf{A}_{x,x';\epsilon} \tau^j \mathbf{A}_{x',x;\epsilon'} \} = \\ & = \nu^2 \text{tr} \begin{bmatrix} e^{i\epsilon(x-x')} & s\Theta_{r-\epsilon} e^{i\epsilon(x+x') + is\phi_s(\epsilon)} \\ s\beta^i \Theta_{r-\epsilon} e^{-i\epsilon(x+x') - is\phi_s(\epsilon)} & \beta^i e^{-i\epsilon(x-x')} \end{bmatrix} \\ & \times \begin{bmatrix} e^{-i\epsilon'(x-x')} & s\Theta_{r-\epsilon'} e^{i\epsilon'(x+x') + is\phi_s(\epsilon')} \\ s\beta^j \Theta_{r-\epsilon'} e^{-i\epsilon'(x+x') - is\phi_s(\epsilon')} & \beta^j e^{i\epsilon'(x-x')} \end{bmatrix} \\ & = \nu^2 \left(\mathcal{A}_{\epsilon,\epsilon'}^{ij}(x - x') + \beta^i \Theta_{r-\epsilon} \Theta_{r-\epsilon'} \mathcal{A}_{\epsilon,\epsilon'}^{ij}(x + x' + s\ell_s) \right) \end{aligned} \quad (\text{A4})$$

where we used the approximation (3.6) for the reflection phase shifts.

When substituting the above expressions for the trace into Eq. (A1), it is convenient to define

$$F_r(x) = \nu^2 \int_r^\infty d\epsilon d\epsilon' \frac{f(\epsilon) - f(\epsilon')}{i\Omega_n - (\epsilon - \epsilon')} e^{i(\epsilon-\epsilon')x/v}. \quad (\text{A5})$$

Note that in both cases, *after* evaluating the trace, the conditions $\epsilon > r$ and $\epsilon' > r$, or $\epsilon < r$ and $\epsilon' < r$, enter simultaneously. Hence the polarization operator (A1) can be expressed via (A5) as

$$\begin{aligned} \Pi_{x,x';\Omega_n}^{ij} &= \\ &= \frac{1 - ss'}{2} [F_r(x - x' + s\ell_t) + \beta^i \beta^j F_r(x' - x - s\ell_t)] \\ &+ \frac{1 + ss'}{2} \left\{ \Pi_{x,x';\Omega_n}^{(0)ij} \right. \\ &\left. + \beta^j [F_{-r}(x + x' + s\ell_s) + \beta^i \beta^j F_{-r}(-x' - x - s\ell_s)] \right\}. \end{aligned} \quad (\text{A6})$$

The last term is obtained from Eq. (A5) via the interchange of the dummy variables $\epsilon \rightarrow -\epsilon'$ and $\epsilon' \rightarrow -\epsilon$, and using $f(-\epsilon) = 1 - f(\epsilon)$. We also define the polarization operator in the translation-invariant case

$$\Pi_{x,x';\Omega_n}^{(0)ij} = [F_r(x - x') + \beta^i \beta^j F_r(x' - x)]_{r \rightarrow -\infty}. \quad (\text{A7})$$

We now proceed to evaluating (A5). Introducing the variable $\varepsilon = \epsilon - \epsilon'$, write

$$\begin{aligned} F_r(x) &= \nu^2 \int_r^\infty d\epsilon \int_{-\infty}^{\epsilon-r} d\varepsilon \frac{f(\epsilon) - f(\epsilon - \varepsilon)}{i\Omega_n - \varepsilon} e^{i\varepsilon x/v} \\ &= \nu^2 \int_{-\infty}^0 \frac{e^{i\varepsilon x/v} d\varepsilon}{i\Omega_n - \varepsilon} \int_r^\infty d\epsilon [f(\epsilon) - f(\epsilon - \varepsilon)] \\ &+ \nu^2 \int_0^\infty \frac{e^{i\varepsilon x/v} d\varepsilon}{i\Omega_n - \varepsilon} \int_{r+\varepsilon}^\infty d\epsilon [f(\epsilon) - f(\epsilon - \varepsilon)]. \end{aligned} \quad (\text{A8})$$

The integration with respect to ϵ and ε is over a domain that can be split into an infinite rectangle, $\epsilon > r$ and $\varepsilon < 0$, and an infinite triangle, $\epsilon > r$ and $0 < \varepsilon < \epsilon - r$. After changing the order of integration in each of the two sub-domains separately, such that the integral over ϵ is performed first, one obtains the last equation in (A8). Shifting variables in the energy integrations and introducing the function

$$\varphi(\varepsilon) = \int_r^{r+\varepsilon} d\epsilon f(\epsilon) = \varepsilon + T \ln \frac{f(r + \varepsilon)}{f(r)}, \quad (\text{A9})$$

we get

$$F_r(x) = \nu^2 \int_0^\infty d\varepsilon \varphi(\varepsilon) \left[\frac{e^{i\varepsilon x/v}}{\varepsilon - i\Omega_n} + \frac{e^{-i\varepsilon x/v}}{\varepsilon + i\Omega_n} \right]. \quad (\text{A10})$$

Consider first the static part, $F_r^{\text{stat}}(x) \equiv F_r(x)|_{i\Omega_n=0}$; it can be represented as

$$F_r^{\text{stat}}(x) = \nu f(r) \delta_B(x) \quad (\text{A11})$$

where $\delta_B(x)$ is a function with a peak at $x = 0$ that carries unit weight, $\int dx \delta_B(x) \equiv 1$. In the limit $r \rightarrow -\infty$, the function δ_B reduces to a delta function; in the classical limit, $0 < r/T \ll 1$, the peak has a width of order $\xi_T = v/T$.

The dynamic part of the F_r function, $F_r^{\text{dyn}} \equiv F_r - F_r^{\text{stat}}$,

$$F_r^{\text{dyn}}(x) = \nu^2 i\Omega_n \int_0^\infty d\varepsilon \frac{\varphi(\varepsilon)}{\varepsilon} \left[\frac{e^{i\varepsilon x/v}}{\varepsilon - i\Omega_n} - \frac{e^{-i\varepsilon x/v}}{\varepsilon + i\Omega_n} \right] \quad (\text{A12})$$

is dominated by the poles, $\varepsilon = \pm i\Omega_n$. The leading behavior

$$F_r^{\text{dyn}}(x) \simeq -\pi \nu^2 \Omega_n f(r) [\text{sign } x + \text{sign } \Omega_n] e^{-|\Omega_n x|/v} \quad (\text{A13})$$

originates from the odd part $\varphi(\varepsilon) \rightarrow \varphi_- = \frac{1}{2}[\varphi(\varepsilon) - \varphi(-\varepsilon)] = \varepsilon f(r) + \mathcal{O}(\varepsilon^3)$ by extending the integral over to the real axis and evaluating the Taylor-expanded $\varphi_-(\varepsilon)$. The even part, $\varphi_+ = \frac{1}{2}[\varphi(\varepsilon) + \varphi(-\varepsilon)]$, and the higher-order terms of the odd part, yield the corrections $\mathcal{O}(f'(r)\Omega_n^2 \log |\Omega_n x|)$ that are subleading in the dc limit, $\omega/T \ll 1$, of small real frequencies, $i\Omega_n \rightarrow \omega + i0$ after the analytic continuation.

We now have all the ingredients to construct the polarization operator (A6). First, the absolute values of the arguments of the F_r functions in (A6) are all larger than the scattering lengths ℓ_\pm that characterize the length of the Mott region of the wire. In the limit of a long Mott wire, $\ell_\pm T/v \gg 1$ we can neglect the tails of the static part (A11) of the F_r functions in (A6). The static part then only enters the polarization via the contribution $\Pi^{(0)ij}$ which was defined in (A7). The F_r functions in (A6) thus only contribute with their dynamic part (A13). Moreover, for the dynamic part the scattering lengths ℓ_\pm in the arguments of the F_r functions in (A6) can be effectively set to zero as they give only subleading corrections in the dc limit $\omega \ell_\pm/v \ll 1$. After these simplifications we finally obtain the expression (3.12) for the polarization operator.

-
- ¹ M. P. A. Fisher and L. I. Glazman, in *Mesoscopic Electron Transport*, NATO Advanced Studies Institute, Series E: Applied Science, edited by G. S. L. Kouwenhoven and L. Sohn (Kluwer Academic, Dordrecht, 1997).
- ² C. L. Kane and M. P. A. Fisher, Phys. Rev. B **46**, 15233 (1992).
- ³ D. L. Maslov and M. Stone, Phys. Rev. B **52**, 5539(R) (1995).
- ⁴ V. V. Ponomarenko, Phys. Rev. B **52**, 8666(R) (1995).
- ⁵ I. Safi and H. J. Schulz, Phys. Rev. B **52**, 17040(R) (1995).
- ⁶ O. Starykh and D. L. Maslov, Phys. Rev. Lett. **80**, 1694 (1998).
- ⁷ M. Mori, M. Ogata, and H. Fukuyama, J. Phys. Soc. Jpn. **66**, 3363 (1997); see also the slightly extended version cond-mat/9708002(v1).
- ⁸ T. Giamarchi, *Quantum Physics in One Dimension* (Oxford University Press, Oxford, 2004).
- ⁹ S. Tarucha, T. Honda, and T. Saku, Solid State Commun. **94**, 413 (1995).
- ¹⁰ K. A. Matveev, Phys. Rev. Lett. **92**, 106801 (2004).
- ¹¹ L.I. Glazman, G.B. Lesovik, D.E. Khmelnitskii, and R.I. Shekhter, Pis'ma Zh. Exp. Teor. Fiz. **48**, 218 (1988) [Sov. Phys. JETP Lett. **48** (1988) 238]; see also the review by C. W. J. Beenakker and H. van Houten, in *Solid State Physics*, edited by H. Ehrenreich and D. Turnbull (Academic, New York, 1991), Vol. 44, p. 1.
- ¹² A. Luther and V. J. Emery, Phys. Rev. Lett. **33**, 589 (1974).
- ¹³ X. Zotos, J. Phys. Soc. Jpn., Suppl. v.74, p.173 (2005).
- ¹⁴ M. Garst and A. Rosch, Europhys. Lett. **55**, 66 (2001).
- ¹⁵ K. Damle and S. Sachdev, Phys. Rev. Lett. **95**, 187201 (2005).
- ¹⁶ B. L. Altshuler, R. M. Konik, A. M. Tsvelik, Nucl. Phys. B **739**, 311 (2006).
- ¹⁷ T. Giamarchi, Phys. Rev. B **44**, 2905 (1991).
- ¹⁸ G. I. Japaridze and A. A. Nersesyan, JETP Lett. **27**, 334.
- ¹⁹ V. L. Pokrovsky and A. L. Talapov, Phys. Rev. Lett. **42**, 65 (1979).
- ²⁰ S. Coleman, Phys. Rev. D **11**, 2088 (1975).
- ²¹ F. D. M. Haldane, J. Phys. A **15**, 507 (1982).
- ²² The bare gap Δ in the Hamiltonian (2.7) is renormalized by the interactions. The details of such renormalization are not important; here we assume that the tuning parameter (1.1) is defined with respect to the renormalized Δ .
- ²³ D. S. Fisher and P. A. Lee, Phys. Rev. B **23** 6851 (1981).
- ²⁴ We evaluate the measurable conductance, which is defined as a current response to the externally applied electric field, see Refs. 3,4,5. This definition differs from that of Y. Oreg and A. M. Finkel'stein, Phys. Rev. B **54**, R14265 (1996) and A. Kawabata, J. Phys. Soc. Jpn. **65**, 30 (1996).
- ²⁵ E. B. Kolomeisky, Phys. Rev. B **47**, 6193 (1993).
- ²⁶ K. A. Matveev, D. Yue, and L. I. Glazman, Phys. Rev. Lett. **71**, 3351 (1993).
- ²⁷ D. Yue, L. I. Glazman, and K. A. Matveev, Phys. Rev. B **49**, 1966 (1994).
- ²⁸ Y. V. Nazarov and L. I. Glazman, Phys. Rev. Lett. **91**, 126804 (2003).
- ²⁹ L. P. Kouwenhoven, F. W. Hekking, B. J. van Wees, C. J. P. M. Harmans, C. E. Timmering, and C. T. Foxon, Phys. Rev. Lett. **65**, 361 (1990).

- ³⁰ V. I. Talyanskii, D. S. Novikov, B. D. Simons, and L. S. Levitov, Phys. Rev. Lett. **87**, 276802 (2001); D. S. Novikov, Phys. Rev. B **72**, 235428 (2005).
- ³¹ Y. V. Nazarov and D. V. Averin, Phys. Rev. Lett. **81**, 653 (1998).
- ³² R. Klesse and A. Stern, Phys. Rev. B **62**, 16912 (2000); T. Fuchs, R. Klesse and A. Stern, Phys. Rev. B **71**, 045321 (2005).